ABSTRACT

DNA damage occurs in many settings, including normal replication and exposure to radiation. Branched DNA structures such as Holliday junctions (HJs) and 5' flaps are important intermediates formed in the process of DNA repair, and *H. sapiens* GEN1 is a nuclease that can repair these intermediates. *In vitro,* human GEN1 and the structurally similar *Drosophila melanogaster* GEN (*Dm*GEN) cleave 5' flaps more efficiently than HJs. Substrate specificity is thought to be determined by a helical arch region, adjacent to the active site, through which ssDNA may be threaded for cleavage. Homologs of GEN have variable arch regions, and thus different substrate specificities— while *Dm*GEN has specificity for HJs, 5' flaps, and replication forks, its ortholog from *C. thermophilum* (*Ct*GEN1) lacks the arch region, and thus is limited to HJ activity. Conversely, its homolog found in *H. sapiens* (*Hs*FEN1) exhibits specificity for 5' flaps due to a different arch region. To manipulate the substrate specificity of *Dm*GEN, I replaced the arch region with the corresponding region from both *Ct*GEN1 and *Hs*FEN1 to yield two chimeric proteins termed $GEN^{[CtGEN1]}$ and $GEN^{[HsFEN1]}$. I hypothesized that $GEN^{[CtGEN1]}$ would have specificity to only HJs and $GEN^{[HsFEN1]}$ would have specificity only to 5' flaps. Nuclease assays revealed that neither $GEN^{[CtGEN1]}$ nor $GEN^{[HsFEN1]}$ was able to cleave HJs, suggesting that the swapped region plays a role in substrate binding or cleavage. Further research, including 5' flap nuclease assays and *in vivo* experiments, is needed to better understand the consequences of only cleaving 5' flaps or HJs in DNA repair. Ultimately, this work will offer novel insights into the role of the *Dm*GEN nuclease including its substrate specificity in isolation and in the greater context of DNA damage repair pathways in *Drosophila* and humans alike.

INTRODUCTION

DNA is routinely damaged by factors such as UV radiation, carcinogens, errors in the normal replication pathway, and recombination. If damage persists, cells may undergo apoptosis or exhibit cancerous growth, two fates that can be catastrophic. During normal DNA repair in response to damage, branched DNA structures are formed, such as Holliday junctions (HJs), 5' flaps, splayed arms, and forked structures that serve as intermediates (Holliday 1964; Ishikawa et al. 2004; Kanai et al. 2007; Ip et al. 2008). A unique class of nucleases termed structure-specific endonucleases is responsible for cleaving and thus resolving these branched DNA intermediates. *Drosophila melanogaster* GEN (*Dm*GEN) is an endonuclease shown to have affinity for HJs and is thus termed a HJ resolvase (Ip et al. 2008). *In vitro* studies have shown that *Dm*GEN and its human ortholog are also able to resolve branched and forked structures that arise in the DNA damage repair process (Ip et al. 2008; Chan and West 2015; Bellendir et al. 2017).

Though the activity of *H. sapiens* GEN1 is important in the DNA repair pathway, it has been shown that GEN functions secondarily to Mus81 in humans and yeast (Blanco et al. 2010; Tay and Wu 2010; Muñoz et al. 2012; Sarbajna et al. 2014). This relationship is reversed in *Drosophila melanogaster; Gen* mutants exhibit more sensitivity to damaging agents than *mus81* mutants, suggesting that *Dm*GEN assumes a primary role in resolving damaged DNA (Andersen et al. 2011; Bellendir et al. 2017). While it was previously understood that the main function of *Dm*GEN was as a HJ resolvase (Ip et al. 2008), our lab has recently shown that *in vitro,* both human and *Drosophila* GEN

act more efficiently on 5' flaps, a ssDNA substrate (Bellendir et al. 2017; Figure 1). The contradiction between the recent biochemical data and the genetic data sparks an interesting question: what is the most critical DNA intermediate to resolve *in vivo*? *Drosophila melanogaster* is a useful model in which to answer this due to its use of *Dm*GEN as a primary enzyme in DNA repair. Because *Dm*GEN is primary and cleaves 5' flaps most effectively, we hypothesize that resolving these simpler branched structures may be the more biologically important activity of GEN and its orthologs in repairing damaged DNA.

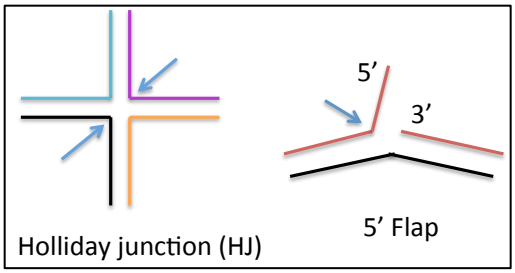

Figure 1. HJ and 5' flap substrates.
Blue arrows correspond to the site of cleavage by GEN and homologous nucleases. On the HJ substrate, cleaving across the other diagonal is equally as likely.

Interestingly, the substrate specificity of GEN homologs varies depending on the organism. This inconsistency can be attributed to a highly variable region within residues 76-151 of GEN homologs (Tomlinson et al. 2010; Bellendir et al. 2017; Figure 2). This region corresponds to an arch in the protein, which is adjacent to its active site (Lee et al. 2015; Liu et al. 2015). This arch is thought to be responsible for threading ssDNA through for better cleavage (Ceska et al. 1996; Patel et al. 2012). *Dm*GEN has the arch, yet is able to act on HJs, 5' flaps, replication forks, and splayed arms (Kanai et al. 2007; Bellendir et al. 2017). Its ortholog *C. thermophilum* GEN1 (*Ct*GEN1) acts strictly on HJs (Liu et al. 2015; Bellendir et al. 2017) and accordingly lacks the arch

region (Lilley 2017; Figure 3). Its structurally similar homolog found in *H. sapiens*, *Hs*FEN1, plays a similar role in damage repair, yet shows specificity for 5' flaps (Patel et al. 2012). While *Hs*FEN1 has an arch, it is structured differently than that of *Dm*GEN1 and thus exhibits 5' flap substrate specificity (Rass et al. 2010; Tsutakawa et al. 2011; Patel et al. 2012).

```
DmGEN: VLEGVAPKLKSQVIAKRNELQFRGVKP---KNSPECTQSQPSKGDKGR---SRFNHVLKQCETLLLSMGIQ :136
HsFEN1: VFDGKPPQLKSGELAKRSERRAEAEKQ---LQQAQAAGAEQEVEKFTKRLVKVTKQHNDECKHLLSLMGIP :151
CtGEN1: VFDG-----PNKPIFKRNRRSGTGNGV---STAX------------------------AKRLIRLFGFT :112
```

Figure 2. Protein sequence alignment of *Dm*GEN, *Hs*FEN1, and *Ct*GEN1

The amino acids highlighted in blue, red, and orange represent the arch region swapped out of *Dm*GEN and replaced with that of either *Hs*FEN1 or *Ct*GEN1. Note the large stretch of amino acids that is missing in *Ct*GEN1—this corresponds to it lacking the arch region. Image adapted from Bellendir et al. 2017.

Figure 3. Protein overlay of *Dm*GEN and *Ct*GEN1

Pymol generated overlay of *Ct*GEN1 (PDB: 5CNQ) crystal structure with PHYRE generated protein model of *Dm*GEN. *Dm*GEN (light pink) and *Ct*GEN1 (fuchsia). The arch in *Dm*GEN is indicated with an arrow, which is absent in *Ct*GEN1.

We aim to further investigate the substrate specificity of *Dm*GEN and its role in DNA damage repair. We proposed to alter its substrate specificity from HJs, 5' flaps, and forked DNA to solely HJs or 5' flaps in two separate experiments. In doing so, we effectively "limited" the DNA intermediates *Dm*GEN acts on. This was done by replacing a 60-residue span of *Dm*GEN (its arch region) with the corresponding regions from *Ct*GEN1 and *Hs*FEN1 in two separate experiments. By doing so, the two chimeric proteins are expected to exhibit altered substrate specificities; the protein with the 50-residue region from *Ct*GEN1 (termed $GEN^{[CtGEN1]}$) is expected to show specificity for HJs, and the protein with the region from *Hs*FEN1 (termed $GEN^{[HsFEN1]}$) is expected to show specificity for 5' flaps. We hypothesize that altering this crucial region is sufficient to alter the substrate specificity of GEN and allow us to isolate its activity on one substrate or the other in the context of WT *Dm*GEN.

Here, we show purified $GEN^{[HsFEN1]}$ and $GEN^{[CtGEN1]}$ with an altered substrate specificity from that of WT *Dm*GEN. However, instead of acting only on HJs, the chimeric $GEN^{[CtGEN1]}$ does not show specificity for HJs *in vitro*. As hypothesized, $GEN^{[HsFEN1]}$ also does not exhibit HJ activity.

MATERIALS AND METHODS

A. Plasmid construction

Both GEN$^{[CtGEN1]}$ and GEN$^{[HsFEN1]}$ were created using IDT gBlocks® Gene Fragments to synthesize the sequences from *CtGen1* and *HsFen1*. These sequences were first codon-optimized for expression in bacterial cells using the IDT Codon Optimization Tool; *E. coli* are biased towards certain codons, so this was taken into account for both fragments, as they would eventually be expressed in *E. coli.* The sequences were inserted into the parental vector pET21b-tr-Gen-His, which contains a truncated and more stable *DmGen* (1-518 amino acids), as well as a hexahistidine tag used in purification (Bellendir et al. 2017; Figure 4). pET21b-tr-Gen-His was linearized using 1 U each of *SmaI* and *MfeI*. The *CtGen1* and *HsFen1* sequences were amplified via PCR using primers with overhangs complementary to the restriction enzyme sites *SmaI* and *MfeI* in the pET21b-tr-Gen-His vector. The sequences were then inserted into the linear pET21b-tr-Gen-His using In-Fusion cloning. Once verified by restriction enzyme digest, 5 µL of pET21b-tr-Gen-His-CtGEN1 and 5 µL of pET21b-tr-Gen-His-HsFEN1 were transformed into Mach1 chemically competent *E. coli* cells for DNA amplification. The transgenic DNA was purified through alkaline lysis. The plasmids were verified using 1 U of *SmaI* and *MfeI* in a diagnostic restriction enzyme digest and subsequent sequencing.

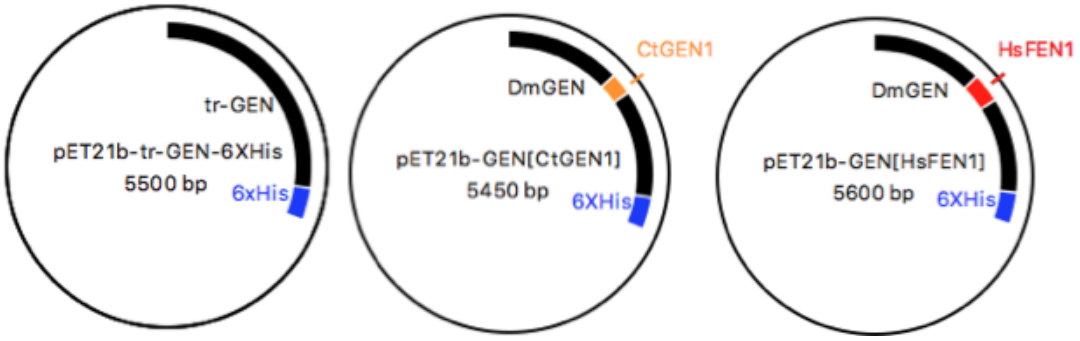

Figure 4. Plasmid construction
Plasmid representations of the wild type *DmGen* (left) from pET21b-tr-Gen-His used as a template, as well as the transgenic plasmids containing $DmGen^{[CtGEN1]}$ (orange) and $DmGen^{[HsFEN1]}$ (red). The sequence for *CtGen1* is slightly smaller than that of *HsFen1*, corresponding to its lacking the arch region. Generated using Plasmidomics 0.2.

B. Protein expression

5 µL of plasmids containing $DmGen^{[CtGEN1]}$ and $DmGen^{[HsFEN1]}$ were each transformed into 50 µL Rosetta pLysS *E. coli* bacterial cells (Novagen), which are optimized for eukaryotic protein expression. The cells were heat shocked at 42°C for 30 seconds and allowed to recover on ice for 30 minutes. Following recovery, 500 µL Luria Broth (LB) media was added to each transformation tube and left to shake for 1 hour incubated at 37°C. 300 µL of the transformation reactions were plated on ampicillin plates. After overnight growth at 37°C, one colony of each transformation reaction was isolated for incubation in 10 mL LB shaking for 16 hours at 37°C. All 10 mL of each overnight culture was added to two separate beveled flasks containing 1 L LB and 1 mL ampicillin resistance each for large-scale expression. Both 1 L flasks were incubated, shaking at 37°C for 4 hours until the optical density (OD_{600}) reached 0.4. The OD_{600} measures the absorbency of the bacteria at 600 nm wavelength, which thus indicates its concentration. The temperature of the incubator was then turned down to 18°C, allowing

the temperature to slowly get cooler and reach 18°C when the OD_{600} was at 0.72 for the bacteria expressing $GEN^{[CtGEN1]}$ and 0.8 for $GEN^{[HsFEN1]}$. An OD_{600} within a range of 0.6-0.8 indicates that the bacteria have reached a density optimal for protein expression induction. To induce protein expression, 0.01 mM of IPTG was added to each 1 L flask. IPTG activates the lac operon, which drives expression of proteins in the Rosetta pLysS cells, thus expressing the chimeric proteins. Both cells expressed at 18°C for 18 hours. After 18 hours, the cells were spun down at 4500 RPM at 4°C for 30 minutes. The supernatant was discarded, and the cell pellets were frozen at -20°C until protein purification.

C. Protein purification

$GEN^{[HsFEN1]}$ and $GEN^{[CtGEN1]}$ were purified separately using the same protocol for each (Bellendir et al. 2017). The N-terminal hexahistidine tag on $GEN^{[HsFEN1]}$ and $GEN^{[CtGEN1]}$ has an imidazole side with an affinity for Ni^{+2}, so the tagged proteins were first passed through a nickel column. $GEN^{[HsFEN1]}$ and $GEN^{[CtGEN1]}$ were resuspended in NiA buffer (20 mM KH_2PO_4 pH7.0, 100 mM ammonium acetate, 1mM DTT, 500 mM NaCl, 50 mM imidazole) and sonicated to break open the cell membrane, making the proteins accessible for purification. The supernatant was loaded onto a 5mL HisTrap HP column (GE Healthcare Life Sciences, Pittsburgh, PA). They were then eluted off the column using NiB buffer (20 mM KH_2PO_4 pH 7.0, 100 mM ammonium acetate, 1 mM DTT, 500 mM NaCl, 500 mM imidazole). For ion exchange purification, a 6 mL Resource S column (GE Healthcare Life Sciences) was first equilibrated with MonoSA buffer (20 mM KH_2PO_4 pH 7.0, 100 mM ammonium acetate, 1 mM DTT, 50 mM NaCl). The peak

eluted proteins from the HisTrap HP column were diluted to 50 mM in NiA buffer without salt (20 mM KH_2PO_4 pH 7.0, 100 mM ammonium acetate, 1 mM DTT) and loaded onto the cation exchange column. The pI measurements of $GEN^{[HsFEN1]}$ and $GEN^{[CtGEN1]}$ are 8.9 and 8.6, respectively (compared to a pI from WT tr-GEN of 8.83). Because the pI of both chimeric proteins is greater than the pH of the buffer (7.0), the protein is positive in solution and thus the cation column was used. The proteins that bound to the cation column were eluted with increasing MonoSB (20 mM KH_2PO_4 pH 7.0, 100 mM ammonium acetate, 1mM DTT, 1 M NaCl). The peak fractions were added to a Superdex S200 column (GE Healthcare Life Sciences) for size exclusion chromatography. $GEN^{[CtGEN1]}$ and $GEN^{[HsFEN1]}$ were eluted using S200 buffer (50 mM HEPES, 400 mM NaCl, 100 mM ammonium acetate, 1 mM DTT) and frozen for storage at -80°C.

D. Western Blot

100 and 250 ng concentrations of $GEN^{[CtGEN1]}$ and $GEN^{[HsFEN1]}$ were run on an SDS-PAGE and transferred overnight to the membrane at 4°C. The membrane was incubated with the primary antibody (rabbit-α-GEN, 1:40,000 dilution) at 25°C for 1 hr. The membrane was washed for 1 hr with 1X PBST. The secondary antibody (α-rabbit-goat, 1:5,000 dilution) was added and incubated with the membrane for 45 minutes shaking at 25°C. After washing in 1X PBST, the membranes were exposed to 1 mL of a chemiluminescent substrate for detection (ThermoFisher SuperSignal Chemiluminescent Substrates). The membrane was exposed to film for 1 second and subsequently developed (Figure 6).

E. Nuclease Assay

Purified GEN$^{[CtGEN1]}$ and GEN$^{[HsFEN1]}$, as well as WT tr-*Dm*GEN as a positive control were each diluted to 2 μM, and fluorescently-labeled HJ substrate was diluted to 229 nM (WT *Dm*GEN and HJ substrate gifts of Matthew Satusky). The three proteins were incubated in three separate 21 μL reactions each containing 90% Master HJ Mix [30% glycerol, 8.14 μL reaction buffer (50 mM Tris pH 8, 100 ug/mL BSA, 1mM DTT, 50 mM KCl, 5 mM $MgCl_2$)] and 1% HJ substrate (229 nM) and allowed to react. Time points of the reactions were taken at 0, 10, 30, 60, 120, 300, and 600 seconds following initial incubation. The reactions were stopped by removing 3 μL aliquots of each and mixing with 6 μL deproteinization buffer (1.25 mg/mL ProK, 1.25% SDS, 62.5 mM EDTA). After 15 minutes of deproteinization, 9 μL of loading buffer was added to the 9 μL of deproteinized reactions, and all 18 μL were loaded onto an 8% native gel and allowed to run at 200 V for 1.5 hours.

Results

Purified GEN$^{[CtGEN1]}$ and GEN$^{[HsFEN1]}$ are expected sizes

It remains unknown whether the arch region is sufficient to confer substrate specificity to *Dm*GEN and its homologs. In attempt to investigate this, the helical arch region of *Dm*GEN was swapped out and replaced with the corresponding regions from *Ct*GEN1 and *Hs*FEN1. To validate the sizes, an SDS-PAGE of the purified proteins was first run. Wild-type truncated *Dm*GEN is ~58 kDa (Bellendir et al. 2017), so because GEN$^{[CtGEN1]}$ lacks the arch, it is slightly smaller at 56 kDa. Conversely, GEN$^{[HsFEN1]}$ is slightly larger

than WT truncated *Dm*GEN at 60 kDa. The SDS-PAGE demonstrates the expected sized bands of GEN$^{[CtGEN1]}$ and GEN$^{[HsFEN1]}$ (Figure 5). Notable in Figure 5 are the very faint bands underneath each darker top band. Those most likely correspond to degraded protein, which would still be GEN and thus not eliminated by the purification steps.

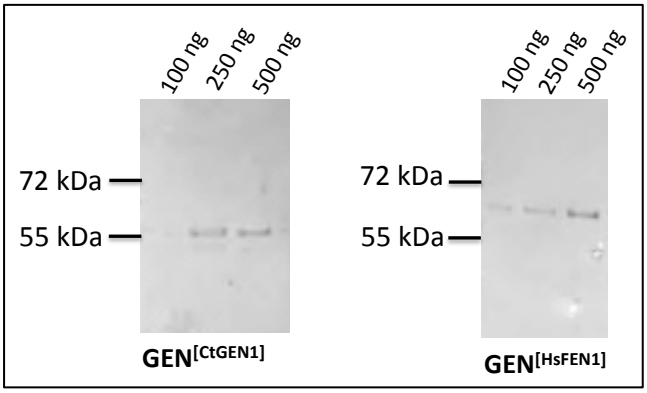

Figure 5. SDS-PAGE of GEN$^{[CtGEN1]}$ and GEN$^{[HsFEN1]}$

Both chimeric proteins on a 12% SDS-PAGE with increasing concentrations stained with Coomassie. GEN$^{[CtGEN1]}$ is about 56 kDa in size and GEN$^{[HsFEN1]}$ is about 60 kDa in size.

GEN$^{[CtGEN1]}$ and GEN$^{[HsFEN1]}$ are visible on western blot

To ensure that the proteins seen in Figure 5 are in fact GEN, an antibody to GEN was used to perform a western blot. In both lanes with 250 ng of loaded protein, as well as the lane containing 100 ng of loaded GEN$^{[HsFEN1]}$, there are visible degradation products to which the GEN antibody bound, confirming that the faint lower band in the SDS-PAGE is indeed GEN. Nuclease-dead versions of WT tr-*Dm*GEN have been made according to this protocol, and have confirmed that all activity is due to the mutated protein, in our case GEN$^{[CtGEN1]}$ or GEN$^{[HsFEN1]}$ (Bellendir et al. 2017). The degradation products are about 30 and 40 kDa in size for GEN$^{[HsFEN1]}$ and about 40 and 53 kDa for GEN$^{[CtGEN1]}$. The difference between the two concentrations of loaded protein in the GEN$^{[HsFEN1]}$ samples is much more noticeable than the difference between the two

concentrations of GEN[CtGEN1], as the GEN[HsFEN1] 250 ng sample is much more overexposed. Nevertheless, this western confirms the presence of purified GEN[HsFEN1] and GEN[CtGEN1], and explains the lower bands present on the SDS-PAGE gel are due to degradation product.

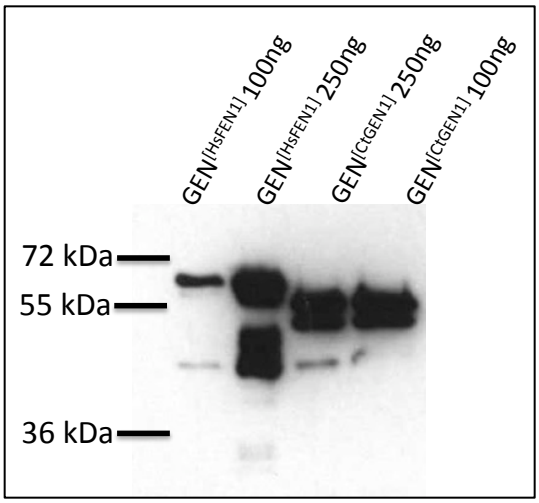

Figure 6. Western blot of GEN[HsFEN1] and GEN[CtGEN1].
The western blot of GEN[HsFEN1] and GEN[CtGEN1]. Full- length products are visible at ~60 kDa and ~56 kDa for GEN[HsFEN1] and GEN[CtGEN1], respectively. Degraded product is visible at ~30 and ~40 kDa for GEN[HsFEN1] and ~40 and ~53 kDa for GEN[CtGEN1].

Nuclease assay reveals GEN[HsFEN1] and GEN[CtGEN1] inactivity on HJs

A nuclease assay was used to test the activity of GEN[CtGEN1] and GEN[HsFEN1] *in vitro* on the HJ substrate (provided by Matthew Satusky). Wild-type DmGEN cleaves HJs bidirectionally and thus yields three products; as the intact HJ decreases in concentration, the three fluorescently-labeled products increase in concentration (Panel A, Figure 7). These bands are not observed with GEN[HsFEN1] or GEN[CtGEN1] – the lower three HJ products are notably absent while the intact HJ remains constant, indicating that those proteins did not act on the HJ substrate.

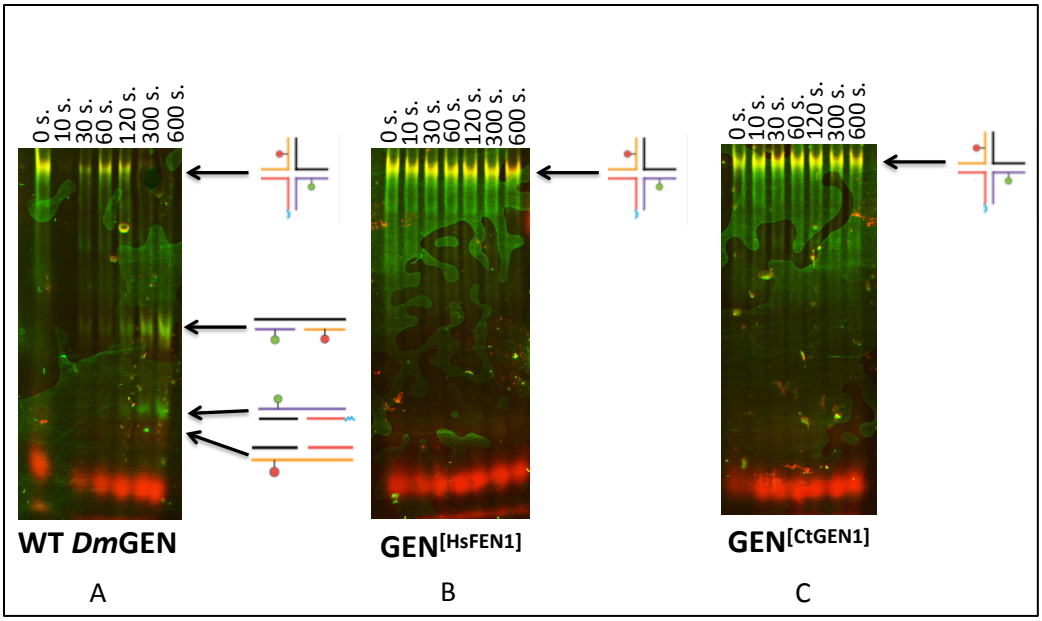

Figure 7. Nuclease assay for *in vitro* Holliday junction activity

Above, nuclease assay with representation of tagged Holliday junction and in panel A, possible cleavage products. Panels B and C show no observable activity of the chimeric proteins on the HJ substrate. Note: the 10-second timepoint in panel A lacks observable data and this is most likely due to the reaction being loaded incorrectly or not at all.

DISCUSSION AND CONCLUSION

The importance of HJ versus 5' flap substrate resolution *in vivo* still remains unknown in DNA damage repair. Here, we used *Drosophila melanogaster* GEN to test this due to its role as the primary enzyme in the repair pathway (Andersen et al. 2011, Bellendir et al. 2017). Two *Dm*GEN-based chimeric proteins were generated, which were predicted to have altered substrate specificity. *In vitro,* these proteins were hypothesized to act on either HJs or 5' flaps *in vitro*. Our *in vitro* nuclease assays reveal that both chimeric proteins, GEN$^{[HsFEN1]}$ and GEN$^{[CtGEN1]}$, do not show HJ activity. This is to be expected for GEN$^{[HsFEN1]}$, due to its arch region conferring specificity for 5' flap substrates. However, GEN$^{[CtGEN1]}$ was expected to show activity on HJs due to the HJ resolvase activity of the

host organism's *Ct*GEN1. Yet, the chimeric protein GEN$^{[CtGEN1]}$ does not have observable activity on HJs in this assay.

This could be attributed to a number of factors. While *Ct*GEN1 is structurally similar to *Dm*GEN, it lacks the arch region and thus is limited to the four-way branched junctions (Lilley 2017). We hypothesized that swapping just the ~50 residue region from *Ct*GEN1 into the arch region of *Dm*GEN (and thus eliminating *Dm*GENs arch region) would be sufficient to confer the HJ substrate specificity of *Ct*GEN1. However, it is possible that the active site or protein structure of the host protein is necessary for substrate binding or cleavage; the arch region of *Ct*GEN1 may not exhibit HJ specificity outside of the context of the *Ct*GEN1 protein. It is also possible that in changing that portion of the protein, we inhibited certain interactions responsible for protein dimerization on HJs, the proteins were unable to dimerize, and thus unable to act on HJs (Bellendir et al. 2017). It is unlikely that protein denaturation is causing the inactivity of GEN$^{[CtGEN1]}$, as it was handled the same as WT *Dm*GEN throughout the experiment.

Future goals include testing the protein activity on 5' flaps and *in vivo* experiments. The 5' flap *in vitro* nuclease assays will also be tested using fluorescently-labeled substrates as was done to test for HJ specificity. We hypothesize that GEN$^{[HsFEN1]}$ will have activity on 5' flaps and appear similar to the *Dm*GEN control, as *Dm*GEN can also cut flapped substrates. We do not expect to see GEN$^{[CtGEN1]}$ activity on 5' flaps because this protein should not have the arch used for threading flapped DNA through.

Assuming that GEN$^{[HsFEN1]}$ acts on 5’ flaps *in vitro*, this protein will be a useful tool *in vivo* in *Drosophila melanogaster*. It will allow us to investigate consequences or benefits of having substrate specificity for solely flapped structures. Endogenous GEN will be replaced with the codon-optimized chimeric protein. Flies expressing GEN$^{[HsFEN1]}$ will be treated with DNA damaging agents to test for sensitivity and compared to flies with wild-type GEN given the same DNA damaging treatments. If GEN$^{[HsFEN1]}$ acts solely on 5’ flaps and is able to rescue to wild-type levels after DNA damage, it is indicative of 5’ flaps being the more important substrate to resolve *in vivo*.

Branched structures are critical intermediates in DNA damage repair, as their proper resolution leads to successful DNA reparation, replication, and cell growth. Understanding the endonucleases that resolve these intermediates is central to our knowledge of DNA repair. Using *D. melanogaster* is particularly helpful, as *Dm*GEN assumes a primary role as an endonuclease, and as such, cuts 5’ flaps more efficiently than HJs. This indicates that the resolution of flaps (or simpler DNA lesions) is the more critical function of GEN in DNA repair, which can be tested by *in vitro* nuclease assays and *in vivo* sensitivity assays. We hope to gain novel insights into the role of this endonuclease, the substrates it preferentially cleaves, and how this activity can be understood in the context of DNA damage repair in *Drosophila* and humans alike.

ACKNOWLEDGEMENTS

I would like to thank the Sekelsky lab and all of its members, especially Dr. Jeff Sekelsky, Dr. Danielle Rognstad, and Michaelyn Hartmann for their unconditional help and support. I would like to thank William G. Walton of the Redinbo lab for purifying the proteins and allowing me to help. I would like to thank Matthew Satusky of the Erie lab for providing the HJ substrate, WT *Dm*GEN, figures of HJ cleavage products in Figure 7, and for his assistance on the nuclease assay. Thank you to Dr. Rognstad for the protein overlay image that is Figure 3. Thank you to my writing group, Leno Smith and Falecia Metcalf, for their edits and feedback. I would also like to thank Dr. Amy Shaub Maddox for her mentorship, edits, and support.

REFERENCES

Andersen S.L., Kuo H.K., Savukoski D., Brodsky M.H., Sekelsky J. Three structure-selective endonucleases are essential in the absence of BLM helicase in *Drosophila*. PLoS Genet. 2011; 7:e1002315.

Bellendir S.P., Rognstad D.J., Morris L.P., Zapotoczny G., Walton W.G., Redinbo M.R., Ramsden D.A., Sekelsky J., Erie D.A. Substrate preference of Gen endonucleases highlights the importance of branched structures as DNA damage repair intermediates. *Nucleic Acids Research*. 2017; 45:5333-5348.

Blanco M.G., Matos J., Rass U., Ip S.C., West S.C. Functional overlap between the structure-specific nucleases Yen1 and Mus81-Mms4 for DNA-damage repair in *S. cerevisiae*. DNA Repair (Amst.). 2010; 9:394–402.

Ceska T.A., Sayers J.R., Stier G., Suck D. A helical arch allowing single-stranded DNA to thread through T5 5'-exonuclease. Nature. 1996; 382:90-903.

Chan Y.W., West S.C. GEN1 promotes Holliday junction resolution by a coordinated nick and counter-nick mechanism. Nucleic Acids Res. 2015; 43:10882–10892.

Holliday R. A mechanism for gene conversion in fungi. Genet.Res. 1964; 78:282–304.

Ip S.C., Rass U., Blanco M.G., Flynn H.R., Skehel J.M., West S.C. Identification of Holliday junction resolvases from humans and yeast. Nature. 2008; 456:357–361.

Ishikawa G., Kanai Y., Takata K., Takeuchi R., Shimanouchi K., Ruike T., Furukawa T., Kimura S., Sakaguchi K. DmGEN, a novel RAD2 family endo-exonuclease from *Drosophila melanogaster*. *Nucleic Acids Research*. 2004; 32(21):6251-6259. 0.1093/nar/gkh962.

Kanai Y., Ishikawa G., Takeuchi R., Ruike T., Nakamura R., Ihara A., Ohashi T., Takata K., Kimura S., Sakaguchi K. DmGEN shows a flap endonuclease activity, cleaving the blocked-flap structure and model replication fork. FEBS J. 2007; 274:3914–3927.

Lee S.H., Princz L.N., Klugel M.F., Habermann B., Pfander B., Biertuempfel C. Human Holliday junction resolvase GEN1 uses a chromodomain for efficient DNA recognition and cleavage. eLife. 2015; 4:e12256.

Lilley D.M. Holliday junction-resolving enzymes—structures and mechanisms. *FEBS Letters.* 2017. 10.1002/1873-3468.12529.

Liu Y., Freeman A.D., Declais A.C., Wilson T.J., Gartner A., Lilley D.M. Crystal structure of a eukaryotic GEN1 resolving enzyme bound to DNA. Cell Rep. 2015; 13:2565–2575.

Muñoz-Galvan S., Tous C., Blanco M.G., Schwartz E.K., Ehmsen K.T., West S.C., Heyer W.D., Aguilera A. Distinct roles of Mus81, Yen1, Slx1-Slx4, and Rad1 nucleases in the repair of replication-born double-strand breaks by sister chromatid exchange. Mol. Cell. Biol. 2012; 32:1592–1603.

Patel N., Atack J.M., Finger L.D., Exell J.C., Thompson P., Tsutakawa S.E., Tainer J.A., Williams D.M., Grasby J.A. Flap endonucleases pass 5′-flaps through a flexible arch using a disorder-thread-order mechanism to confer specificity for free 5′-ends. *Nucleic Acids Research*. 2012;40(10):4507-4519.

Rass U., Compton S.A., Matos J., Singleton M.R., Ip S.C., Blanco M.G., Griffith J.D., West S.C. Mechanism of Holliday junction resolution by the human GEN1 protein. Genes Dev. 2010; 24:1559–1569.

Sarbajna S., Davies D., West S.C. Roles of SLX1-SLX4, MUS81-EME1, and GEN1 in avoiding genome instability and mitotic catastrophe. Genes Dev. 2014; 28:1124–1136.

Tay Y.D., Wu L. Overlapping roles for Yen1 and Mus81 in cellular Holliday junction processing. J. Biol. Chem. 2010; 285:11427–11432.

Tomlinson C.G., Atack J.M., Chapados B., Tainer J.A., Grasby J.A. Substrate recognition and catalysis by flap endonucleases and related enzymes. Biochemical Society Transactions. 2010; 38:433-437.

Tsutakawa S.E., Classen S., Chapados B.R., Arvai A., Finger L.D., Guenther G., Tomlinson C.G., Thompson P., Sarker A.H., Shen B., Cooper P.K., Grasby J.A., Tainer J.A. Human Flap Endonuclease Structures, DNA Double Base Flipping and a Unified Understanding of the FEN1 Superfamily. *Cell*. 2011; 145:198-211.